# Tunable Rashba spin-orbit coupling and its interplay with multiorbital effect and magnetic ordering at oxide interfaces

Weilong Kong,[1,2,*] Tong Yang,[2,*] Jun Zhou [●],[3] Yong Zheng Luo,[1] Tao Zhu,[2] Jingsheng Chen [●],[4] Lei Shen,[1] Yong Jiang,[5] Yuan Ping Feng,[2,6,†] and Ming Yang [●][7,‡]

[1]*Department of Mechanical Engineering, National University of Singapore, Singapore 117575, Singapore*
[2]*Department of Physics, National University of Singapore, Singapore 117551, Singapore*
[3]*Institute of Materials Research and Engineering, Agency for Science, Technology and Research (A\*STAR),*
*2 Fusionopolis Way, Innovis 138634, Singapore*
[4]*Department of Materials Science and Engineering, National University of Singapore, Singapore 117575, Singapore*
[5]*School of Electronics and Information Engineering, Tiangong University, Tianjin 300387, China*
[6]*Centre for Advanced Two-Dimensional Materials, National University of Singapore, Singapore 117546, Singapore*
[7]*Department of Applied Physics, The Hong Kong Polytechnic University, Hung Hom, Kowloon, Hong Kong, China*

Complex oxide heterostructures such as the $LaAlO_3/SrTiO_3$ (LAO/STO) interface are paradigmatic platforms to explore emerging multidegree of freedom coupling and the associated exotic phenomena. In this paper, we reveal the effects of multiorbital and magnetic ordering on Rashba spin-orbit coupling (SOC) at the LAO/STO (001) interface. Based on first-principles calculations, we show that the Rashba spin splitting near the conduction band edge can be tuned substantially by the interfacial insulator-metal transition due to the varied multiorbital effect of the lowest Ti-3$d$ $t_{2g}$ bands. We further unravel an interplay between Rashba SOC and intrinsic magnetism, in which the Rashba SOC-induced spin polarization is suppressed significantly by the presence of interfacial magnetic ordering. These results deepen our understanding of SOC-related intricate electronic and magnetic reconstruction at the perovskite oxide interfaces and shed light on engineering of oxide heterostructures for all-oxide-based spintronic devices.

## I. INTRODUCTION

The essential feature of spin-orbit coupling (SOC) is that electrons in crystals experience an effective magnetic field in their frame of motion which couples the spin and orbital motion of electrons [1]. The Rashba type of SOC emerges at crystal surfaces or interfaces where the inversion symmetry is broken. It induces spin-momentum locking (**k**-dependent spin polarization) and lifts the spin degeneracy of electronic energy bands (Rashba spin splitting) [2–4]. These properties of Rashba SOC are appealing in spintronic devices, as they facilitate manipulation of the electron spins without the need of an external magnetic field and even enhance the interconversion between charge and spin currents through Edelstein and inverse Edelstein effects [5–7].

Oxide interfaces are promising candidates for spin-orbit-based control of spintronic devices owing to moderate Rashba SOC and long spin lifetime [6]. A well-known example of oxide interfaces is the $LaAlO_3/SrTiO_3$ (LAO/STO) (001) interface, which exhibits LAO-thickness-dependent emergent properties that are absent in the bulk counterparts. These include insulator-metal transition [8–10], high-mobility electron gas [11,12], superconductivity [13,14], and an interfacial

magnetic phase [15–17]. Particularly, gate-tunable Rashba SOC was observed at the LAO/STO interface [18,19], which has been used to demonstrate the interconversion between spin and charge currents [17,20–22]. Further studies found that the efficiency of the spin-to-charge conversion was dependent on Rashba SOC strength and spin lifetime [6,20,23,24]. Due to longer spin lifetime, the conversion efficiency of the LAO/STO interface is even higher than that of systems with heavier elements like Bi/Ag interfaces or topological insulators such as $Bi_2Se_3$ [6,23,25]. Additionally, Rashba SOC at the LAO/STO interface has led to many exotic properties, including skyrmions [26,27], topological superconductivity [28], and the intrinsic spin Hall effect [29]. Thus, the LAO/STO interface offers us a unique playground to explore Rashba SOC effects and their potential device applications.

For bulk STO, the conduction band edge is contributed by the degenerate Ti-3$d$ $t_{2g}$ ($d_{xy}$, $d_{xz}$, and $d_{yz}$) orbitals at the $\Gamma$ point. In contrast, the conduction band edge of the LAO/STO (001) interface is mainly derived from the $d_{xy}$ band. This lifted degeneracy between the $d_{xy}$ and the $d_{yz}/d_{xz}$ bands is due to the broken inversion symmetry and confinement effect [3,30,31]. Consequently, it was found that the $d_{xy}$ band and the $d_{yz}/d_{xz}$ bands of the LAO/STO interface have different effects on Rashba SOC. The Rashba SOC near the bottom of the $d_{xy}$ band takes a phenomenological linear-in-**k** form: $\mathbf{H_R} = \alpha_R(\mathbf{k} \times \boldsymbol{\sigma}) \cdot \mathbf{z}$, where the coefficient $\alpha_R$ indicates the Rashba SOC strength, $\boldsymbol{\sigma}$ denotes a vector of Pauli spin

---

*These authors contributed equally to this work.
†phyfyp@nus.edu.sg
‡mingyang@polyu.edu.hk, kevin.m.yang@polyu.edu.hk

matrices, and **z** is a unit vector normal to the interface [3,30–33]. In contrast, for the $d_{yz}/d_{xz}$ bands, Rashba SOC is cubically dependent on **k**, which even shows an anisotropic behavior [34]. It has been suggested theoretically that the Rashba SOC at the LAO/STO interface can be explained by the SOC and interorbital hopping between $t_{2g}$ orbitals [3,30,31,35,36], wherein the crossing of multiple $t_{2g}$ bands induces strong SOC and interorbital hopping (multiorbital effect), which contributes to large Rashba SOC at the band crossing region [3,30,31,35,36]. Experimentally, it was found that the Rashba SOC strength $\alpha_R$ at the LAO/STO interface is related to carrier density which is tunable by an external electric field [18,19,36,37]. Additionally, it was reported that the orbital character at the conduction band edge of the LAO/STO (001) interface can be tuned from $d_{xy}$ to $d_{yz}/d_{xz}$ by an in-plane (parallel to the interface) biaxial compressive strain [38], which in turn changes the relationship between Rashba SOC and **k**.

The electronic properties of the LAO/STO interface are highly dependent on the LAO thickness, in which insulator-metal transition occurs when the LAO thickness is larger than the critical thickness [e.g., 4 unit cells (uc) for the LAO/STO (001) interface]. Although the Rashba SOC-assisted spin-to-charge conversion at the LAO/STO interface has been demonstrated at different LAO thicknesses (2–40 uc) [17,20–22], the evolution of Rashba SOC with the LAO thickness is still not well understood. In addition to the electronic phase transition, an emerging ferromagnetism has been reported at the conducting LAO/STO interface [39,40], which induces spin polarization. However, it is not clear how this spin polarization affects the Rashba SOC at the LAO/STO interface. Thus, in this paper, we performed comprehensive first-principles calculations to investigate these effects on Rashba SOC at the LAO/STO (001) interface. We find that the Rashba SOC strength near the conduction band edge decreases as the interface undergoes an insulator-metal transition with the increase of LAO thickness. This tendency is ascribed to the dependence of the multiorbital effect on the LAO thickness. Moreover, we show that Rashba SOC is suppressed by the emerging ferromagnetism at the conducting LAO/STO interface.

## II. COMPUTATIONAL DETAILS

All calculations were performed using the density-functional-theory-based Vienna *Ab initio* Simulation Package (VASP 5.4.4.18) with the Perdew-Burke-Ernzerhof (PBE) functional for the electron exchange-correlation interaction [41–43], and the projector augmented wave (PAW) method for the interaction between valence electrons and core ions [44]. Scalar relativistic effects are also included in the PAW method [45]. The onsite Coulomb interactions of Ti $3d$ orbitals and La $4f$ orbitals were considered by using the PBE + U method [46]. Here, $U = 5.0$ eV and $J_H = 0.64$ eV were used for Ti $3d$ orbitals [47,48]. A Hubbard $U$ of 11.0 eV and a $J_H = 0.0$ eV were used for localized $4f$ orbitals of La to push them to a higher energy position [49]. The plane-wave basis with a cutoff energy of 500 eV was used to expand the electronic wave functions. Here, $\Gamma$-centered $k$-point grids for sampling the first Brillouin zone were set to $12 \times 12 \times 12$ and $12 \times 12 \times 1$ for

bulk STO (LAO) and slab models of LAO/STO heterostructures, respectively. A series of slab models $(LAO)_m/(STO)_6$ with LaO/TiO$_2$ interfaces [see Fig. 1(a)] were used in calculations to study the effect of the LAO thickness, where the thickness of the STO substrate was fixed to 6 uc to simulate the STO substrate, and the thickness of LAO layers was denoted by $m$ uc [11,50]. Here, $m$ takes 2, 3, 4, 6, and 8 to capture the insulator-metal transition and thickness effect of the LAO/STO interface. For each slab model, the bottom of the STO substrate was terminated with a TiO$_2$ sublayer to avoid the artificial states induced by the bottom SrO layers [51]. To minimize the interaction between neighboring surfaces, a vacuum layer with a thickness of >20 Å was applied along the $z$ direction (out of plane). All atoms except those of the bottom TiO$_2$ sublayer were fully relaxed until the force acting on each atom was <0.02 eV/Å. The convergence criteria of the total energy was set to $1.0 \times 10^{-6}$ eV. The in-plane lattice parameter of the heterostructure was fixed to that of the optimized STO bulk (3.970 Å), which is consistent with previous calculations and the experimentally reported 3.905 Å [10,11,16]. To avoid the spurious electric field, dipole corrections were applied along the $z$ direction as well [52]. The decoupling of Rashba SOC and ferromagnetism at the conducting LAO/STO interfaces was conducted by calculating SOC included band structures with the charge density from non-spin-polarized self-consistent calculations, in which the magnetic moment on Ti sites was set to 0 $\mu_B$.

## III. RESULTS AND DISCUSSIONS

With the increase of the LAO thickness, the LAO/STO interface undergoes an insulator-metal transition at the critical thickness of 4 uc, accompanied by the emergence of interfacial ferromagnetism (see Figs. S1 and S2 in the Supplemental Material [53]). The coexistence of the ferromagnetism and Rashba SOC at the conducting LAO/STO interface makes it complicated to analyze the evolution of Rashba SOC with the LAO thickness, as both the Rashba SOC and the interfacial ferromagnetism induce spin polarization and lift spin degeneracy. To gain a clear understanding of their roles and interplay, we focus first on the evolution of Rashba SOC with the LAO thickness by leaving out the interfacial ferromagnetism in calculations. After that, we include both the Rashba SOC and the interfacial ferromagnetism and discuss the interplay between Rashba SOC and the interfacial ferromagnetism at the conducting LAO/STO interface.

### A. Evolution of Rashba SOC with the increase of LAO thickness

Figures 1(b) and 1(c) show SOC-included band structures along $\Gamma - X$ ($\frac{\pi}{a}$, 0, 0) ($a$ is the in-plane lattice parameter) of the $(LAO)_3/(STO)_6$ and $(LAO)_6/(STO)_6$ (001) heterostructures, which are representatives of insulating and conducting LAO/STO interfaces, respectively. For the two band structures, both conduction band edges are contributed by the $d_{xy}$ orbital. A crossing between the $d_{xy}$ and $d_{yz}$ bands is noticeable near the conduction band edge, as shown in the zoom-in view in Fig. 1(b). The Rashba SOC-induced spin polarization was analyzed by projecting spins of electrons along $x$, $y$, and $z$ directions. It is found that, for both insulating and
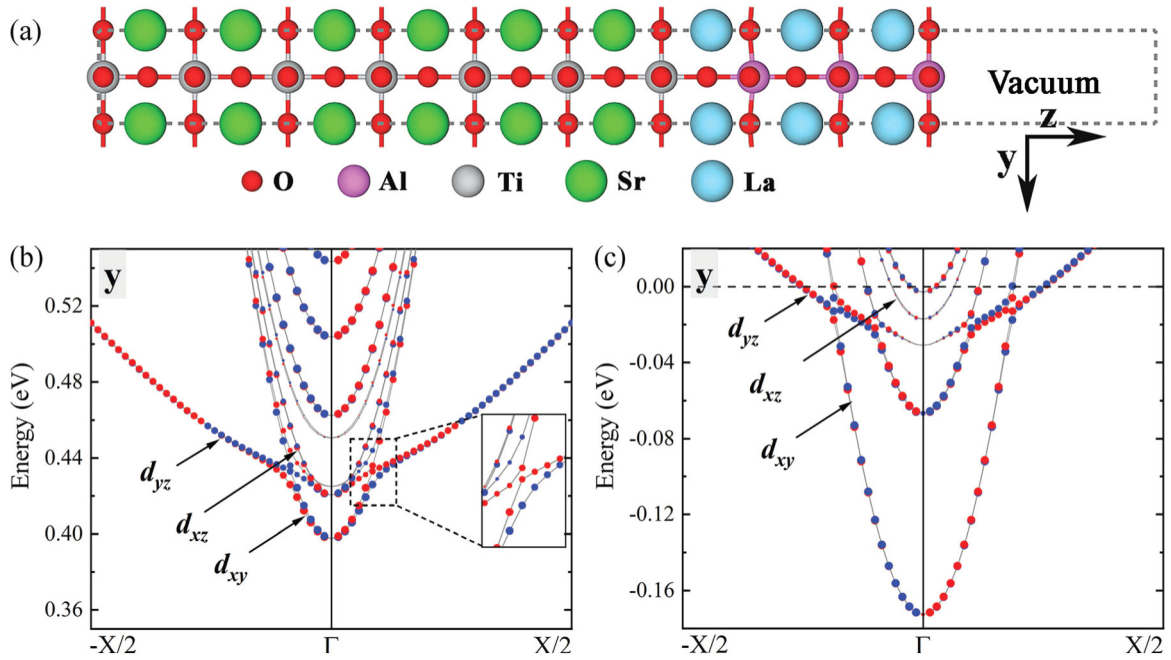
FIG. 1. (a) A schematic diagram of the slab model for the $(LAO)_3/(STO)_6$ heterostructure. Spin-orbit coupling (SOC) included band structures of (b) the $(LAO)_3/(STO)_6$ and (c) $(LAO)_6/(STO)_6$ heterostructures with the projection of electron spins along the $y$ direction, wherein the lowest $t_{2g}$ bands are indicated. Red and blue dots denote positive and negative components of spin projections, respectively. The inset in (b) is a zoom-in view of the crossing region of the lowest $d_{xy}$ and $d_{yz}$ bands.

conducting LAO/STO interfaces, the spins are dominantly polarized along the $y$ direction, which is perpendicular to the selected **k** path along the $\Gamma$-$X$ direction. In contrast, the components of spins along the $x$ and $z$ directions are zero (see Fig. S3 in the Supplemental Material [53]). Figure 2(a) shows a **k**-dependent spin splitting ($\Delta_R$) near the conduction band edge (**k** path from $-X/25$ to $X/25$), which is a zoom-in view of the lowest $d_{xy}$ band in Fig. 1(b). The **k**-dependent spin polarization is a feature of Rashba SOC.

Figure 2(b) shows the evolution of Rashba spin splitting ($\Delta_R$) near the bottom of the lowest $d_{xy}$ band (at the $X/25$) with respect to the LAO thickness. It can be seen that $\Delta_R$ at the

$X/25$ decreases with the increase of the LAO thickness from 2 to 8 uc, especially at the thickness of 4 uc at which the interfacial insulator-metal transition occurs. This trend suggests that the Rashba SOC near the conduction band edge of the insulating interface is stronger than that of the conducting interface. Further analysis reveals that the tendency of $\Delta_R$ in Fig. 2(b) is relevant to the multiorbital effect of the multiple $t_{2g}$ bands [3,36]. In principle, the multiorbital effect is correlated to both SOC and interorbital hopping [3,30,31,35]. At the crossing region of multiple $t_{2g}$ bands, SOC is prominent. This is because, at this region, the SOC strongly mixes the orbitals and couples the spin and orbital degrees of freedom pronouncedly [36].
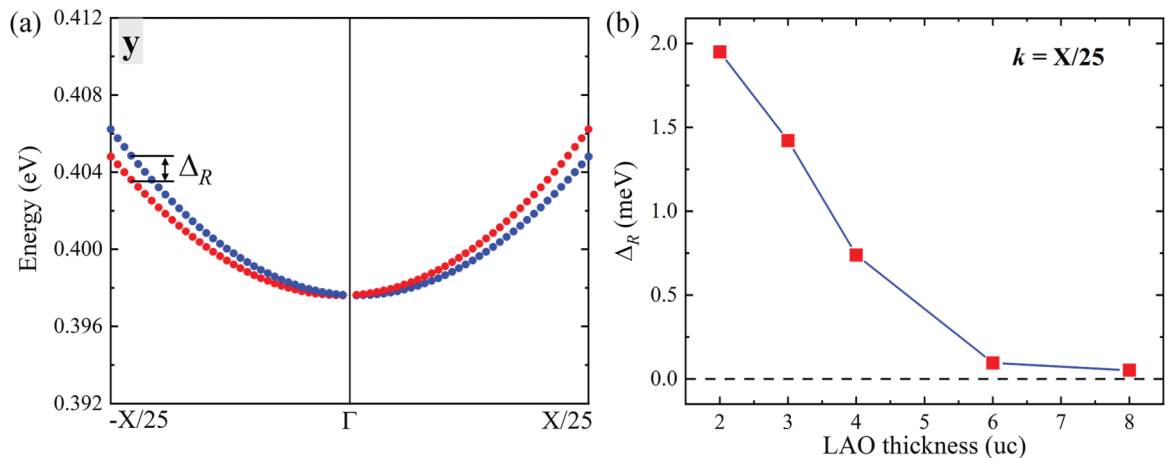


FIG. 2. (a) Rashba spin splitting ($\Delta_R$) near the bottom of the lowest $d_{xy}$ band of the $(LAO)_3/(STO)_6$ heterostructure, where red and blue dots denote positive and negative components of spin projections of the electronic states along the $y$ direction, respectively. The size of the dot indicates the projected weight of the corresponding spin component. (b) The LAO-thickness-dependent $\Delta_R$ of the lowest $d_{xy}$ band at the $X/25$.
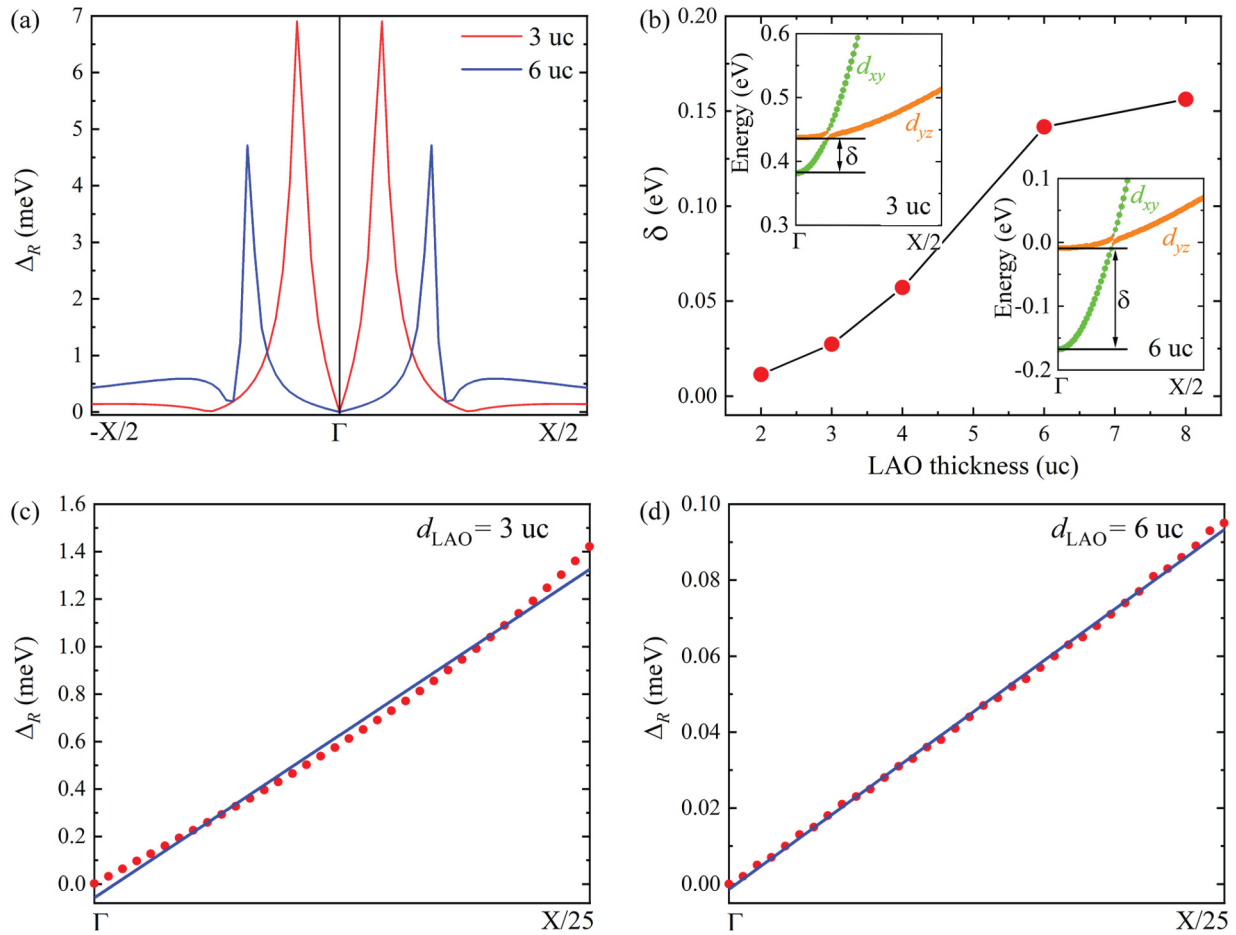
FIG. 3. (a) Rashba spin splitting ($\Delta_R$) of the lowest $d_{xy}$ conduction (a mixture of $d_{xy}$ and $d_{yz}$) band along the $k$-path from $-$X/2 to X/2 for the $(LAO)_3/(STO)_6$ (red solid line) and $(LAO)_6/(STO)_6$ (blue solid line) heterostructure. (b) Variation of the interface-induced orbital splitting $\delta$ between the lowest $d_{xy}$ and $d_{yz}$ bands at the $\Gamma$ point for LAO/STO heterostructures with different LAO thicknesses, in which the insets highlight the $\delta$ in the zoom-in band structures of $(LAO)_3/(STO)_6$ and $(LAO)_6/(STO)_6$ heterostructures, respectively. $\Delta_R$ from the $\Gamma$ point to the X/25 of the lowest $d_{xy}$ band for (c) $(LAO)_3/(STO)_6$ and (d) $(LAO)_6/(STO)_6$ heterostructures are shown by red dotted lines, respectively. The blue lines in (c) and (d) denote the linear fitting of the $\Delta_R$.

Additionally, the interorbital hopping at the band crossing region is strong [30]. Thus, the multiorbital effect leads to large Rashba SOC at the band crossing region [3,30,31,35,36]. The multiorbital-effect-induced large enhancement of $\Delta_R$ is demonstrated in Fig. 3(a), where the maximum $\Delta_R$ of up to several meV occurs at the $k$-points $\sim \pm$X/12 and $\pm$X/6 for insulating [red solid line, $(LAO)_3/(STO)_6$] and conducting [blue solid line, $(LAO)_6/(STO)_6$] interfaces, respectively. These $k$-points correspond to the crossing region of the lowest $d_{xy}$ and $d_{yz}$ bands of the two interfaces. The enhanced $\Delta_R$ at the band crossing region is consistent with previous studies [3,36]. In contrast, $\Delta_R$ decreases dramatically for the $k$-points that are not at the band crossing regions due to the vanishing multiorbital effect. Figure 3(a) also reveals that the maximum $\Delta_R$ at the insulating interface [6.9 meV, $(LAO)_3/(STO)_6$] is larger than that at the conducting interface [4.7 meV, $(LAO)_6/(STO)_6$]. This suggests a stronger multiorbital effect at the band crossing region of the insulating interface.

Additionally, the position of the band crossing region is highly dependent on the band configuration at the LAO/STO interface. Due to the symmetry breaking and confinement effect at the interface, the lowest $d_{xy}$ band splits from the $d_{yz}$

band at the $\Gamma$ point with an energy difference of $\delta$, as shown in Fig. 3(b). The $\delta$ is correlated to the distance between the band crossing region and the bottom of the lowest $d_{xy}$ band. With the increase of LAO thickness, $\delta$ becomes larger [see Fig. 3(b)], as the lowest $d_{xy}$ band is pushed toward a lower energy position by the insulator-metal transition accompanied charge transfer [51]. In this case, the band crossing region moves away from the bottom of the lowest $d_{xy}$ band. Therefore, the multiorbital effect near the bottom of the lowest $d_{xy}$ band is stronger at the insulating LAO/STO interface than that at the conducting LAO/STO interface. This explains why $\Delta_R$ at the X/25 decreases with the increase of the LAO thickness, as observed in Fig. 2(b). The increase of the Rashba SOC near the conduction band edge with the decrease of $\delta$ is consistent with previous tight-binding modeling, where the Rashba SOC strength around the edge of the lowest $d_{xy}$ band was shown inversely proportional to $\delta$ based on perturbative descriptions [3,30].

In addition to the Rashba spin splitting, the LAO-thickness-dependent multiorbital effect also influences the relationship between Rashba SOC and **k** near the bottom of the lowest $d_{xy}$ band. To examine this effect, we have plotted the **k**-dependent

$\Delta_R$ near the bottom of the lowest $d_{xy}$ band for both insulating and conducting interfaces in Figs. 3(c) and 3(d), respectively. For the insulating LAO/STO interface, since its band crossing region is close to the bottom of the lowest $d_{xy}$ band (smaller $\delta$), the dependence of the $\Delta_R$ near the bottom of the lowest $d_{xy}$ band on **k** is found nonlinear [see Fig. 3(c)], resulting from the stronger multiorbital effect. For the conducting interface, its band crossing region is away from the bottom of the lowest $d_{xy}$ band (larger $\delta$). Therefore, $\Delta_R$ is expected to be small and can be fitted linearly dependent on **k**, as shown in Fig. 3(d). In the conducting case, the Rashba coefficient $\alpha_R$ along the $x$ direction is obtained by fitting the $\Delta_R$ to the phenomenological linear-in-**k** Rashba SOC [3]:

$$\Delta_R = 2\alpha_R k_x. \tag{1}$$

The $\alpha_R$ is estimated to be $\sim 1.5\,\mathrm{meV \cdot \mathring{A}}$ for the $(LAO)_6/(STO)_6$ heterostructure, which is in line with previous reports that $\alpha_R$ is in the range from several to tens of meV Å for STO-based heterostructures [3,18,31,35].

## B. The interplay between Rashba SOC and interface magnetic ordering

The above analysis does not include the effect of the interface magnetism. However, along with insulator-metal transition above the critical thickness (LAO thickness $\geqslant 4$ uc), the LAO/STO interface energetically favors the ferromagnetic ordering (see Fig. S1 in the Supplemental Material [53]). This interfacial magnetic ordering is mainly contributed by the lowest $d_{xy}$ band (see Fig. S2 in the Supplemental Material [53]) [15,39,49,54]. The interplay between Rashba SOC and ferromagnetism at the conducting interface is discussed below. The Hamiltonian of the interface including both interfacial ferromagnetism and Rashba SOC takes the form [55–57]:

$$H = \frac{\hbar^2 \mathbf{k}^2}{2m^*} + \alpha_R (\mathbf{k} \times \sigma) \cdot z - M\sigma_z, \tag{2}$$

where $m^*$ is the effective mass of an electron, $M$ is half of the ferromagnetism-induced Zeeman splitting energy, and $\sigma_z$ denotes the interfacial ferromagnetism-induced spin component along the $z$ direction (out of plane). Here, we assume that the magnetization is along the $z$ direction for simplicity. The coexistence of ferromagnetism and Rashba SOC leads to two spin-split bands:

$$E_{\pm} = \frac{\hbar^2 \mathbf{k}^2}{2m^*} \pm \sqrt{\alpha_R^2 \mathbf{k}^2 + M^2}. \tag{3}$$

While the ferromagnetism-induced spin polarization is along the $z$ direction, the Rashba SOC-induced spin polarization is in the $x$-$y$ plane (in plane) and perpendicular to **k**. The ferromagnetism and Rashba SOC, therefore, compete on the alignment of spin orientation. The ratio of the spin polarization induced by them can be quantified by

$$\frac{|\sigma_{\parallel}|}{|\sigma_z|} = \frac{|\mathbf{B}_R|}{|\mathbf{B}_{\mathrm{FM}}|}, \tag{4}$$

where $\sigma_{\parallel}$ denotes the Rashba SOC-induced spin component in the $x$-$y$ plane. Here, $\mathbf{B}_R$ and $\mathbf{B}_{\mathrm{FM}}$ correspond to the Rashba

SOC-induced effective magnetic field and that from ferromagnetism, respectively. Figures 4(a) and 4(b) show that the electronic states are mainly spin polarized in the $z$ direction, and the lowest $d_{xy}$ band exhibits a large energy splitting between the two spin channels, indicative of a pronounced Zeeman splitting ($\sim 0.4$ eV). In contrast, the Rashba SOC-induced spin component (along the $y$ direction) is relatively large for bands with smaller Zeeman splitting, i.e., the lowest $d_{yz}$ band, as shown in the inset of Fig. 4(b). Experimentally, the magnetism at the LAO/STO interface is complicated and strongly dependent on the sample preparation conditions [12,49,54,58,59]. Both the in-plane and out-of-plane ferromagnetism have been reported at the LAO/STO interface [13,14,60–62]. While the ferromagnetism-induced spin polarization is along specific easy axes, the Rashba SOC-induced spin polarization is always perpendicular to the **k** of moving electrons. Therefore, the Rashba SOC-induced spin orientation still competes with that induced by the intrinsic ferromagnetism when the magnetic easy axes are in plane.

It has been suggested that the inhomogeneous magnetism in crystals may also contribute to spin splitting [63], as recently demonstrated in antiferromagnetic crystals, such as $MnF_2$ [64,65], wherein the spin degeneracy is lifted by breaking specific symmetry, including the product of time reversal and spatial inversion symmetry, as well as the product of spinor and translation symmetry. At the conducting and ferromagnetic LAO/STO interface, the distribution of the ferromagnetic ordering might be inhomogeneous, which might make another contribution to spin splitting. In our calculations, however, this effect might not be significant since the large Zeeman splitting ($\sim 0.4$ eV) for the $(LAO)_6/(STO)_6$ heterostructure in Fig. 4(a) indicates a highly ordered interfacial ferromagnetism. Further detailed discussions of the inhomogeneous magnetism-induced spin splitting at the oxide interface will be of great interest but is out of the scope of this paper.

We would like to point out that our calculation results are based on the slab models (vacuum/LAO/STO) without point defects, wherein the LAO-thickness-dependent insulator-metal transition is due to the electron transfer from the LAO surface to the interface. This is different from that in some experiments, where the transferred electrons may also be provided by the capping layers or LAO surface reconstruction [10,20–22]. Although Rashba SOC mainly occurs at the interface that is buried under the LAO layers, it can still be manipulated by capping materials or surface reconstruction, as they may influence the critical thickness of the insulator-metal transition and the electron concentration at the interface. Moreover, biaxial strain on the interface can be introduced when growing the LAO/STO heterostructure on different substrates, i.e., LAO substrate [38]. The biaxial strain applied on the LAO/STO interface may tune the Rashba SOC through influencing the band ordering of Ti $t_{2g}$ orbitals at the interface. In addition to the strain effects, point defects like oxygen vacancies, cation vacancies, and antisite defects may also occur in the LAO/STO heterostructure [54,60]. These points defects will influence the electron concentration at the interface and contribute magnetism to the LAO/STO heterostructure, which can further tune the Rashba SOC at the LAO/STO interface. Our results suggest that the electron concentration, band
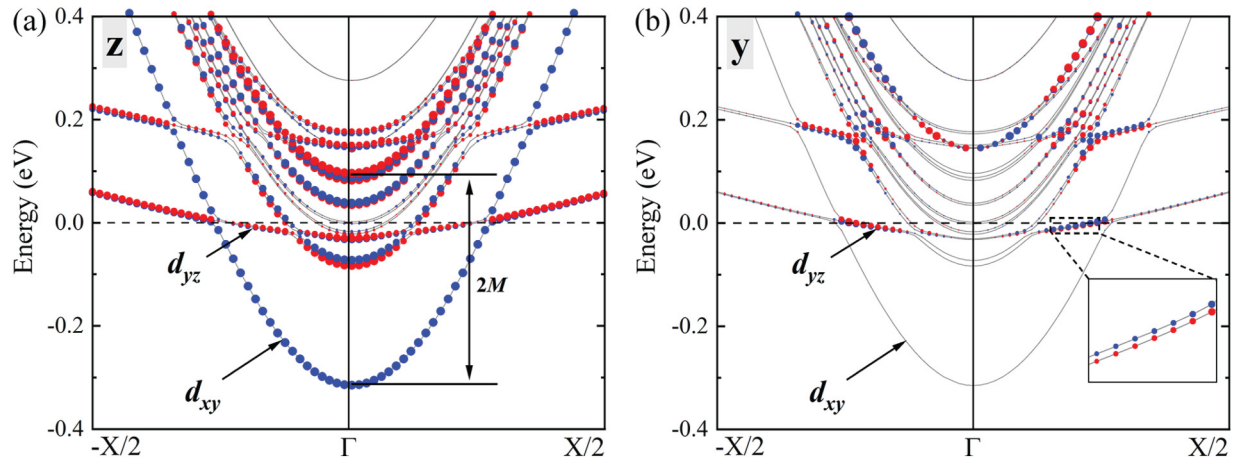
FIG. 4. Band structures of the $(LAO)_6/(STO)_6$ heterostructure including both spin-orbit coupling (SOC) and interface magnetism. (a) and (b) Band structures with the projection of electron spins along $z$ and $y$ directions, respectively. Red and blue solid dots denote positive and negative components, respectively. The size of the dot indicates the projected weight of the corresponding spin component.

ordering relevant multiorbital effect, and magnetic ordering at the interface can be used to manipulate Rashba SOC. Therefore, they can serve as a starting point to study the influence of those specific factors, such as biaxial strain and point defects, on Rashba SOC.

In practical applications, the efficiency of the spin and charge current interconversion is proportional to the strength of the Rashba SOC [20–22]. Based on our calculations, the Rashba SOC near the conduction band edge is inversely proportional to the LAO thickness. Below the critical thickness (4 uc) of the insulator-metal transition, the Rashba SOC in the insulating LAO/STO heterostructures is relatively strong. More importantly, in the insulating LAO/STO heterostructures, the band crossing region with large Rashba spin splitting is closer to the conduction band, which is highly desired as a much lower doping concentration is required to access this band crossing region. In contrast, in the conducting LAO/STO heterostructures, the Rashba SOC is much weaker and barely influenced by the multiorbital effect, as the charge transfer pushes the lowest $d_{xy}$ band toward a lower energy [51]. Additionally, the Rashba SOC-induced spin polarization is suppressed by the charge-transfer-induced interfacial ferromagnetic ordering. Thus, a LAO/STO heterostructure with thinner LAO is more desirable for practical spintronic applications, such as spin-to-charge conversion with the spin pumping technique [20].

### IV. CONCLUSIONS

In conclusion, by using first-principles calculations, we show that the Rashba spin splitting near the conduction band edge of the LAO/STO interface is tunable with the LAO thickness and reveal an interplay between the Rashba SOC and the interface magnetic ordering. With the increase of LAO thickness, the multiorbital-effect-induced enhancement to the Rashba SOC near the conduction band edge decreases as the crossing region of the lowest $d_{xy}$ and $d_{yz}$ bands is gradually away from the bottom of the lowest $d_{xy}$ band. Rashba SOC can be further suppressed by the presence of the ferromagnetism at the conducting LAO/STO interface, in which the spin polarization is dominated by ferromagnetism for bands with large Zeeman splitting. Our results are useful to understand Rashba SOC at the complex oxide interface and highlight that the LAO/STO heterostructure with a thin LAO thickness is more promising for the spintronic applications. This work also serves as an example to further explore Rashba SOC in a rich variety of striking perovskite oxide interfaces.

[1] A. Manchon, H. C. Koo, J. Nitta, S. M. Frolov, and R. A. Duine, New perspectives for Rashba spin-orbit coupling, Nat. Mater. **14**, 871 (2015).

[2] E. I. Rashba, Properties of semiconductors with an extremum loop. I. Cyclotron and combinational resonance in a magnetic field perpendicular to the plane of the loop, Sov. Phys. Solid State **2**, 1109 (1960).

[3] Z. Zhong, A. Tóth, and K. Held, Theory of spin-orbit coupling at LaAlO₃/SrTiO₃ interfaces and SrTiO₃ surfaces, Phys. Rev. B **87**, 161102(R) (2013).

[4] F. T. Vas'ko, Spin splitting in the spectrum of two-dimensional electrons due to the surface potential, Pis'Ma Zh. Eksp. Teor. Fiz. **30**, 574 (1979) [JETP Lett. **30**, 541 (1979)].

[5] Y. P. Feng, L. Shen, M. Yang, A. Wang, M. Zeng, Q. Wu, S. Chintalapati, and C.-R. Chang, Prospects of spintronics based on 2D materials, Wiley Interdiscip. Rev. Comput. Mol. Sci. **7**, e1313 (2017).

[6] J. Varignon, L. Vila, A. Barthélémy, and M. Bibes, A new spin for oxide interfaces, Nat. Phys. **14**, 322 (2018).

[7] V. M. Edelstein, Spin polarization of conduction electrons induced by electric current in two-dimensional asymmetric electron systems, Solid State Commun. **73**, 233 (1990).

[8] S. Thiel, Tunable quasi-two-dimensional electron gases in oxide heterostructures, Science **313**, 1942 (2006).

[9] T. C. Asmara, A. Annadi, I. Santoso, P. K. Gogoi, A. Kotlov, H. M. Omer, M. Motapothula, M. B. H. Breese, M. Rübhausen, T. Venkatesan, Ariando, and A. Rusydi, mechanisms of charge transfer and redistribution in $LaAlO_3/SrTiO_3$ revealed by high-energy optical conductivity, Nat. Commun. **5**, 3663 (2014).

[10] J. Zhou, T. C. Asmara, M. Yang, G. A. Sawatzky, Y. P. Feng, and A. Rusydi, Interplay of electronic reconstructions, surface oxygen vacancies, and lattice distortions in insulator-metal transition of $LaAlO_3/SrTiO_3$, Phys. Rev. B **92**, 125423 (2015).

[11] A. Ohtomo and H. Y. Hwang, A high-mobility electron gas at the $LaAlO_3/SrTiO_3$ heterointerface, Nature (London) **427**, 423 (2004).

[12] X. Wang, Ariando, G. Baskaran, Z. Q. Liu, J. Huijben, J. B. Yi, A. Annadi, A. R. Barman, A. Rusydi, S. Dhar, Y. P. Feng, J. Ding, H. Hilgenkamp, and T. Venkatesan, Electronic phase separation at the $LaAlO_3/SrTiO_3$ interface, Nat. Commun. **2**, 188 (2011).

[13] J. A. Bert, B. Kalisky, C. Bell, M. Kim, Y. Hikita, H. Y. Hwang, and K. A. Moler, Direct imaging of the coexistence of ferromagnetism and superconductivity at the $LaAlO_3/SrTiO_3$ interface, Nat. Phys. **7**, 767 (2011).

[14] L. Li, C. Richter, J. Mannhart, and R. C. Ashoori, Coexistence of magnetic order and two-dimensional superconductivity at $LaAlO_3/SrTiO_3$ interfaces, Nat. Phys. **7**, 762 (2011).

[15] A. Brinkman, M. Huijben, M. van Zalk, J. Huijben, U. Zeitler, J. C. Maan, W. G. van der Wiel, G. Rijnders, D. H. A. Blank, and H. Hilgenkamp, Magnetic effects at the interface between non-magnetic oxides, Nat. Mater. **6**, 493 (2007).

[16] W. Kong, J. Zhou, Y. Z. Luo, T. Yang, S. Wang, J. Chen, A. Rusydi, Y. P. Feng, and M. Yang, Formation of two-dimensional small polarons at the conducting $LaAlO_3/SrTiO_3$ interface, Phys. Rev. B **100**, 085413 (2019).

[17] Y.-Y. Pai, A. Tylan-Tyler, P. Irvin, and J. Levy, Physics of $SrTiO_3$-based heterostructures and nanostructures: a review, Rep. Prog. Phys. **81**, 036503 (2018).

[18] A. D. Caviglia, M. Gabay, S. Gariglio, N. Reyren, C. Cancellieri, and J.-M. Triscone, Tunable Rashba Spin-Orbit Interaction at Oxide Interfaces, Phys. Rev. Lett. **104**, 126803 (2010).

[19] G. Herranz, G. Singh, N. Bergeal, A. Jouan, J. Lesueur, J. Gázquez, M. Varela, M. Scigaj, N. Dix, F. Sánchez, and J. Fontcuberta, Engineering two-dimensional superconductivity and Rashba spin-orbit coupling in $LaAlO_3/SrTiO_3$ quantum wells by selective orbital occupancy, Nat. Commun. **6**, 6028 (2015).

[20] E. Lesne, Y. Fu, S. Oyarzun, J. C. Rojas-Sánchez, D. C. Vaz, H. Naganuma, G. Sicoli, J. Attané, M. Jamet, E. Jacquet, J. George, A. Barthélémy, H. Jaffrès, A. Fert, M. Bibes, and L. Vila, Highly efficient and tunable spin-to-charge conversion through Rashba coupling at oxide interfaces, Nat. Mater. **15**, 1261 (2016).

[21] Q. Song, H. Zhang, T. Su, W. Yuan, Y. Chen, W. Xing, J. Shi, J. Sun, and W. Han, Observation of inverse Edelstein effect in Rashba-split 2DEG between $SrTiO_3$ and $LaAlO_3$ at room temperature, Sci. Adv. **3**, e1602312 (2017).

[22] Y. Wang, R. Ramaswamy, M. Motapothula, K. Narayanapillai, D. Zhu, J. Yu, T. Venkatesan, and H. Yang, Room-temperature giant charge-to-spin conversion at the $SrTiO_3$-$LaAlO_3$ oxide interface, Nano Lett. **17**, 7659 (2017).

[23] J. C. R. Sánchez, L. Vila, G. Desfonds, S. Gambarelli, J. P. Attané, J. M. De Teresa, C. Magén, and A. Fert, Spin-to-charge conversion using Rashba coupling at the interface between non-magnetic materials, Nat. Commun. **4**, 2944 (2013).

[24] K. Shen, G. Vignale, and R. Raimondi, Microscopic Theory of the Inverse Edelstein Effect, Phys. Rev. Lett. **112**, 096601 (2014).

[25] P. Deorani, J. Son, K. Banerjee, N. Koirala, M. Brahlek, S. Oh, and H. Yang, Observation of inverse spin hall effect in bismuth selenide, Phys. Rev. B **90**, 094403 (2014).

[26] S. Banerjee, O. Erten, and M. Randeria, Ferromagnetic exchange, spin-orbit coupling and spiral magnetism at the $LaAlO_3/SrTiO_3$ interface, Nat. Phys. **9**, 626 (2013).

[27] X. Li, W. V. Liu, and L. Balents, Spirals and Skyrmions in Two Dimensional Oxide Heterostructures, Phys. Rev. Lett. **112**, 067202 (2014).

[28] S. Nakosai, Y. Tanaka, and N. Nagaosa, Topological Superconductivity in Bilayer Rashba System, Phys. Rev. Lett. **108**, 147003 (2012).

[29] L. X. Hayden, R. Raimondi, M. E. Flatté, and G. Vignale, Intrinsic spin hall effect at asymmetric oxide interfaces: role of transverse wave functions, Phys. Rev. B **88**, 075405 (2013).

[30] Y. Kim, R. M. Lutchyn, and C. Nayak, Origin and transport signatures of spin-orbit interactions in one- and two-dimensional $SrTiO_3$-based heterostructures, Phys. Rev. B **87**, 245121 (2013).

[31] G. Khalsa, B. Lee, and A. H. MacDonald, Theory of $t_{2g}$ electron-gas Rashba interactions, Phys. Rev. B **88**, 041302(R) (2013).

[32] J. Zhou, W.-Y. Shan, and D. Xiao, Spin responses and effective Hamiltonian for the two-dimensional electron gas at the oxide interface $LaAlO_3/SrTiO_3$, Phys. Rev. B **91**, 241302(R) (2015).

[33] C. S. Ho, W. Kong, M. Yang, A. Rusydi, and M. B. A. Jalil, Tunable spin and orbital polarization in $SrTiO_3$-based heterostructures, New J. Phys. **21**, 103016 (2019).

[34] H. J. Harsan Ma, J. Zhou, M. Yang, Y. Liu, S. W. Zeng, W. X. Zhou, L. C. Zhang, T. Venkatesan, and Y. P. Feng, Giant crystalline anisotropic magnetoresistance in nonmagnetic perovskite oxide heterostructures, Phys. Rev. B **95**, 155314 (2017).

[35] P. D. C. C. King, S. McKeown Walker, A. Tamai, A. de la Torre, T. Eknapakul, P. Buaphet, S.-K. Mo, W. Meevasana, M. S. Bahramy, and F. Baumberger, Quasiparticle dynamics and spin–orbital texture of the $SrTiO_3$ two-dimensional electron gas, Nat. Commun. **5**, 3414 (2014).

[36] A. Joshua, S. Pecker, J. Ruhman, E. Altman, and S. Ilani, A universal critical density underlying the physics of

electrons at the LaAlO$_3$/SrTiO$_3$ interface, Nat. Commun. **3**, 1129 (2012).

[37] C. Yin, P. Seiler, L. M. K. Tang, I. Leermakers, N. Lebedev, U. Zeitler, and J. Aarts, Tuning Rashba spin-orbit coupling at LaAlO$_3$/SrTiO$_3$ interfaces by band filling, Phys. Rev. B **101**, 245114 (2020).

[38] W. Lin, L. Li, F. Doğan, C. Li, H. Rotella, X. Yu, B. Zhang, Y. Li, W. S. Lew, S. Wang, W. Prellier, S. J. Pennycook, J. Chen, Z. Zhong, A. Manchon, and T. Wu, Interface-based tuning of Rashba spin-orbit interaction in asymmetric oxide heterostructures with 3$d$ electrons, Nat. Commun. **10**, 3052 (2019).

[39] J.-S. Lee, Y. W. Xie, H. K. Sato, C. Bell, Y. Hikita, H. Y. Hwang, and C.-C. Kao, Titanium $d_{xy}$ ferromagnetism at the LaAlO$_3$/SrTiO$_3$ Interface, Nat. Mater. **12**, 703 (2013).

[40] K. Michaeli, A. C. Potter, and P. A. Lee, Superconducting and Ferromagnetic Phases in SrTiO$_3$/LaAlO$_3$ Oxide Interface Structures: Possibility of Finite Momentum Pairing, Phys. Rev. Lett. **108**, 117003 (2012).

[41] G. Kresse and J. Hafner, *Ab initio* molecular dynamics for liquid metals, Phys. Rev. B **47**, 558 (1993).

[42] G. Kresse and J. Hafner, *Ab initio* molecular dynamics for open-shell transition metals, Phys. Rev. B **48**, 13115 (1993).

[43] G. Kresse and J. Furthmüller, Efficiency of *ab-initio* total energy calculations for metals and semiconductors using a plane-wave basis set, Comput. Mater. Sci. **6**, 15 (1996).

[44] G. Kresse and D. Joubert, From ultrasoft pseudopotentials to the projector augmented-wave method, Phys. Rev. B **59**, 1758 (1999).

[45] J. Hafner, *Ab-initio* simulations of materials using VASP: density-functional theory and beyond, J. Comput. Chem. **29**, 2044 (2008).

[46] A. I. Liechtenstein, V. I. Anisimov, and J. Zaanen, Density-functional theory and strong interactions: orbital ordering in Mott-Hubbard insulators, Phys. Rev. B **52**, R5467 (1995).

[47] M. Altmeyer, H. O. Jeschke, O. Hijano-Cubelos, C. Martins, F. Lechermann, K. Koepernik, A. F. Santander-Syro, M. J. Rozenberg, R. Valentí, and M. Gabay, Magnetism, Spin Texture, and In-Gap States: Atomic Specialization at the Surface of Oxygen-Deficient SrTiO$_3$, Phys. Rev. Lett. **116**, 157203 (2016).

[48] S. Okamoto, A. J. Millis, and N. A. Spaldin, Lattice Relaxation in Oxide Heterostructures: LaTiO$_3$/SrTiO$_3$ Superlattices, Phys. Rev. Lett. **97**, 056802 (2006).

[49] M. Yang, J. Zhou, Ariando, T. C. Asmara, P. Krüger, X. J. Yu, X. Wang, C. Sanchez-Hanke, Y. P. Feng, T. Venkatesan, and A. Rusydi, Direct observation of room-temperature stable magnetism in LaAlO$_3$/SrTiO$_3$ heterostructures, ACS Appl. Mater. Interfaces **10**, 9774 (2018).

[50] N. Reyren, S. Thiel, A. D. Caviglia, L. F. Kourkoutis, G. Hammerl, C. Richter, C. W. Schneider, T. Kopp, A.-S. Ruetschi, D. Jaccard, M. Gabay, D. A. Muller, J.-M. Triscone, and J. Mannhart, Superconducting interfaces between insulating oxides, Science **317**, 1196 (2007).

[51] W.-J. Son, E. Cho, B. Lee, J. Lee, and S. Han, Density and spatial distribution of charge carriers in the intrinsic $n$-type LaAlO$_3$-SrTiO$_3$ interface, Phys. Rev. B **79**, 245411 (2009).

[52] L. Bengtsson, Dipole correction for surface supercell calculations, Phys. Rev. B **59**, 12301 (1999).

[53] See Supplemental Material at http://link.aps.org/supplemental/10.1103/PhysRevB.104.155152 for details of charge transfer and ferromagnetism at the LAO/STO interface, atom- and orbital-projected band structure of the heterostructure, and SOC included band structures of the heterostructure with the projection of electron spins to $x$ and $z$ directions.

[54] L. Yu and A. Zunger, A polarity-induced defect mechanism for conductivity and magnetism at polar-nonpolar oxide interfaces, Nat. Commun. **5**, 5118 (2014).

[55] K. Rahmanizadeh, G. Bihlmayer, and S. Blügel, Spin-orbit and exchange effects in the 2DEG of BiAlO$_3$-based oxide heterostructures, EPL (Europhysics Lett.) **115**, 17006 (2016).

[56] D. Oshima, K. Taguchi, and Y. Tanaka, Unconventional gate voltage dependence of the charge conductance caused by spin-splitting Fermi surface by Rashba-type spin-orbit coupling, Phys. E: Low-Dimens. Syst. Nanostructures **114**, 113615 (2019).

[57] P. Středa and P. Šeba, Antisymmetric Spin Filtering in One-Dimensional Electron Systems with Uniform Spin-Orbit Coupling, Phys. Rev. Lett. **90**, 256601 (2003).

[58] F. Bi, M. Huang, S. Ryu, H. Lee, C.-W. Bark, C.-B. Eom, P. Irvin, and J. Levy, Room-temperature electronically-controlled ferromagnetism at the LaAlO$_3$/SrTiO$_3$ interface, Nat. Commun. **5**, 5019 (2014).

[59] F. Bi, M. Huang, H. Lee, C.-B. Eom, P. Irvin, and J. Levy, LaAlO$_3$ thickness window for electronically controlled magnetism at LaAlO$_3$/SrTiO$_3$ heterointerfaces, Appl. Phys. Lett. **107**, 082402 (2015).

[60] D. S. Park, A. D. Rata, I. V. Maznichenko, S. Ostanin, Y. L. Gan, S. Agrestini, G. J. Rees, M. Walker, J. Li, J. Herrero-Martin, G. Singh, Z. Luo, A. Bhatnagar, Y. Z. Chen, V. Tileli, P. Muralt, A. Kalaboukhov, I. Mertig, K. Dörr, A. Ernst, and N. Pryds, The emergence of magnetic ordering at complex oxide interfaces tuned by defects, Nat. Commun. **11**, 3650 (2020).

[61] T. D. N. Ngo, J.-W. Chang, K. Lee, S. Han, J. S. Lee, Y. H. Kim, M.-H. Jung, Y.-J. Doh, M.-S. Choi, J. Song, and J. Kim, Polarity-tunable magnetic tunnel junctions based on ferromagnetism at oxide heterointerfaces, Nat. Commun. **6**, 8035 (2015).

[62] B. Kalisky, J. A. Bert, C. Bell, Y. Xie, H. K. Sato, M. Hosoda, Y. Hikita, H. Y. Hwang, and K. A. Moler, Scanning probe manipulation of magnetism at the LaAlO$_3$/SrTiO$_3$ heterointerface, Nano Lett. **12**, 4055 (2012).

[63] S. I. Pekar and E. I. Rashba, Combined resonance in crystals in inhomogeneous magnetic fields, Zh. Eksperim. Teor. Fiz. **47**, 1927 (1964) [Sov. Phys. JETP **20**, 1295 (1965)].

[64] L.-D. Yuan, Z. Wang, J.-W. Luo, E. I. Rashba, and A. Zunger, Giant momentum-dependent spin splitting in centrosymmetric low-$z$ antiferromagnets, Phys. Rev. B **102**, 014422 (2020).

[65] L.-D. Yuan, Z. Wang, J.-W. Luo, and A. Zunger, Prediction of low-$z$ collinear and noncollinear antiferromagnetic compounds having momentum-dependent spin splitting even without spin-orbit coupling, Phys. Rev. Materials **5**, 014409 (2021).